Faster, cheaper, safer optical tweezers for the undergraduate laboratory

John Bechhoefer[a] and Scott Wilson
Department of Physics, Simon Fraser University, Burnaby, British Columbia V5A 1S6, Canada

(Received 22 December 2000; accepted 15 November 2001)

We describe an optical tweezers experiment suitable for a third-year undergraduate laboratory course. Compared to previous designs, it may be set up in about half the time and at one-third the cost. The experiment incorporates several features that increase safety. We also discuss how to use stochastic methods to characterize the trap's strength and shape. © *2002 American Association of Physics Teachers.*

[DOI: 10.1119/1.1445403]

I. INTRODUCTION

A tightly focused beam of light can attract and trap micron-sized dielectric particles whose refractive index exceeds that of the surrounding medium. Although single-beam optical traps were developed only in 1986, they have already proven their worth in making possible an increasing number of experiments.[1] Optical traps have found particular use in biophysics, where they allow one to manipulate single molecules of DNA,[2] allowing one access to their physical properties and to the properties of attached molecules of biological interest. They have been used passively, to record the forces induced on a bead, for example, by kinesin molecules[3] and myosin-V.[4] In other applications, tweezers have played an active role, for example, to induce a ''pearling'' instability in lipid vesicles.[5] The tweezer-induced motion of a bead also can be used to measure local elasticities and viscosities, for example, inside cells.[6]

The first designs of optical tweezers used large ($\geqslant 1$ W) lasers and expensive optical hardware, which placed them beyond the reach of undergraduate laboratories. Recently, however, Smith *et al.*[7] developed an apparatus that is simple and cheap enough to be included in an undergraduate laboratory. This article explores improvements to their original design, the cumulative effect of which is to make the apparatus more practical and much cheaper. In addition, the design eliminates several possibilities for injuries, increasing the safety of the experiment. (After the first version of this work was submitted, Moothoo *et al.* published a design with similarities to ours.[8] There are, nonetheless, a number of differences worth discussing. In addition, a *two-beam* trap using a hollow-core fiber has also been described.[9] It shares some of the advantages of the design described here, although lasers of much higher power are required.)

In the following, we first briefly review the theory of optical tweezers, mostly to alert the reader to a recent theoretical advance that greatly simplifies calculations. We then discuss our design and its rationale, along with a careful discussion of one application for the tweezers.

II. BRIEF REVIEW OF OPTICAL TWEEZER THEORY

The theory for optical tweezers has been extensively discussed, for example, in Ref. 7; however, that discussion considers just two limits, one where the particle radius R is much smaller[10] than the wavelength of light λ and one where $R \gg \lambda$.[11] In the former limit ($R \ll \lambda$), one pictures the particle as a collection of dipoles that are polarized by a slowly varying electric field. (Slowly varying refers to the spatial variation of the envelope, not the fast varations associated with the optical frequency.) The energy of the particle is then

$$W = UV = -\tfrac{1}{2}\alpha\varepsilon_0 E^2 V, \tag{1}$$

where

$$\alpha = \frac{\varepsilon_p}{\varepsilon_0} - 1 \approx \frac{n_p^2}{n_0^2} - 1 \tag{2}$$

takes into account the relative dielectric constants (related, for transparent particles, for optical frequencies to the refractive indices as shown) of the particle and the surrounding medium. In Eq. (1), $V = (4/3)\pi R^3$ is the particle volume and $U = -(1/2)\vec{P}\cdot\vec{E}$ is the local electrostatic energy density, with P the polarization and E the electric field. Because $U \propto E^2$, it is also proportional to the local light intensity I (power/area). Thus, gradients of light intensity lead to gradients in W and hence to forces exerted on the particle. These forces may be found by differentiating the expression for W with respect to the particle coordinates. For $\alpha > 0$ (particle index higher than that of the surrounding medium), there will be an attractive force towards regions of higher intensity. This force allows one to trap dielectric particles near the focus of a microscope objective, where there is a local intensity maximum. If we further consider the destabilizing influence of radiation pressure, we find that we must use high-numerical-aperture objectives to have stable traps; otherwise, radiation pressure pushes the particle downstream, out of a single-beam trap. In practice, we must use oil-immersion objectives with numerical aperture (NA) > 1.

The above discussion assumes $R \ll \lambda$. The other limit, $R \gg \lambda$, may be treated by geometrical optics.[11] The problem is that trapping forces are most effective when $R \approx \lambda$, where neither method is accurate. Recently, Tlusty *et al.*[12] introduced an approach that is valid for arbitrary particle size, assuming only a small index difference between trapping particle and surrounding fluid. (The small-index approximation is valid in the application described below.) They argue that for highly localized beams, there is neglible phase difference across the spot size w and that we can then generalize Eq. (1) to

$$W = -\alpha \int_V \frac{1}{2}\varepsilon_0 E^2 \, dV, \tag{3}$$

and that this expression holds for all particle sizes. Here, the integral is over the particle volume V. They then approxi-

mate the local energy density near the focus of a Gaussian laser beam as

$$U(\rho,z)=U_0\exp\left(-\frac{\rho^2}{2w^2}-\frac{z^2}{2w^2\epsilon}\right), \tag{4}$$

where ρ is the radial distance from the beam axis, z is the distance along the axis, centered on the focus, and $U_0=\frac{1}{2}\varepsilon_0E^2$ is the maximum energy density of the beam (at the focus, $\rho=z=0$). Here, ϵ is the anisotropy of the energy density near the focus. For weakly focused light (NA$\ll$1), $\epsilon\approx$1/NA. For the large numerical apertures used in tweezer experiments, $\epsilon\approx 3$.[12] The somewhat artificial limit of $\epsilon=1$, although not achievable in practice, leads to a simple analytical formula. Thus, for example, Tlusty *et al.*[12] find that for $\epsilon=1$, the linear restoring force on a trapped particle subject to small perturbations is given by

$$k=\alpha U_0 w\frac{4\pi}{3}a^3e^{-a^2/2}, \tag{5}$$

where $a=R/w$ is the particle size relative to the laser beam waist. For the more realistic case of nonzero ϵ, they find[13]

$$k_\rho=\alpha U_0 w\frac{2\pi\epsilon^3}{\xi^3}\left[\sqrt{\frac{\pi}{2}}\left(\left(\frac{\xi a}{\epsilon}\right)^2-1\right)e^{-a^2/2}\,\mathrm{erf}\left(\frac{\xi a}{\sqrt{2}\epsilon}\right)+\left(\frac{\xi a}{\epsilon}\right)e^{-a^2/2\epsilon^2}\right], \tag{6}$$

and

$$k_z=\alpha U_0 w\frac{4\pi\epsilon}{\xi^3}\left[\sqrt{\frac{\pi}{2}}e^{-a^2/2}\,\mathrm{erf}\left(\frac{\xi a}{\sqrt{2}\epsilon}\right)-\left(\frac{\xi a}{\epsilon}\right)e^{-a^2/2\epsilon^2}\right], \tag{7}$$

where $\xi=\sqrt{1-\epsilon^2}$. Tlusty *et al.*[12] show that these expressions, as well as the complete expressions for the nonlinear restoring force on large perturbations are in remarkable agreement with experiments, for all sizes of particles used.

III. OPTICAL TWEEZERS SETUP

Figure 1 shows our version of the optical tweezers. Like other designs, it uses a laser beam that is suitably expanded and shaped and focuses it through a high-NA microscope objective. The objective serves at the same time to make a conventional optical image so that students can see (and find) the trapped object. Our design has, however, a number of original features.

A. Laser

The original laboratory designs were based on ND:YAG or argon ion lasers, costing upwards of $10,000. That of Ref. 7 was based on a 17 mW HeNe laser which costs about $2200. Ours uses a visible diode-laser module costing approximately $500.[14] Although high-power diode lasers, particularly in the infrared, have been available for some time, their poor beam quality has posed an obstacle to using them as sources for optical tweezers. The quality of an optical trap depends on sharply focusing a laser beam to a diffraction-limited spot. A beam shape that deviates markedly from a TEM_{00} Gaussian profile will lead to larger, less efficient traps.

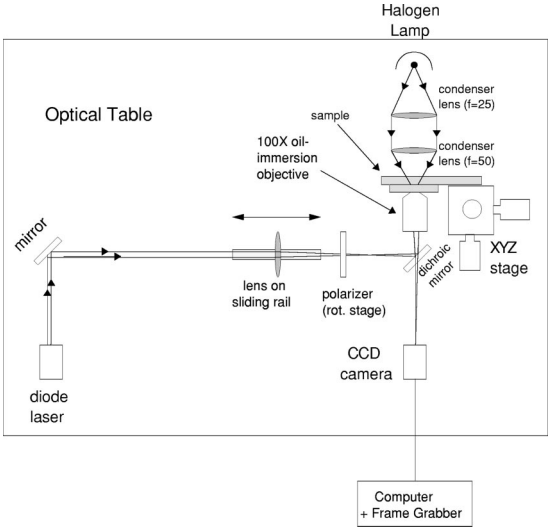

Fig. 1. Optical tweezer setup.

The beam from a diode laser has several problems. First, it may be multimode, which guarantees larger spot sizes. Fortunately, many single-mode lasers are now available. Second, the beam is elliptical, with differing divergence angles along different coordinate axes. These have traditionally been corrected with an anamorphic prism, which is both expensive and adds complexity to the optical path. Third, the beam is astigmatic: different directions seem to originate from points that are displaced axially from each other by as much as a few microns. Without correction, such a beam cannot be focused to a small spot size.

One approach to reducing astigmatism involves blocking all parts of a beam except that which has the required shape. We can, for example, couple the laser into a single-mode optical fiber and use the exiting beam; however, coupling losses reduce considerably the available power, raising that required of the original laser diode.

An alternate approach is to use cylindrical optics to both equalize the divergence angle and to eliminate astigmatism. An implementation of this idea that uses a miniature cylinder implanted in the laser diode case has been introduced by Blue Sky Research.[14] We chose a commercial module based on their modified laser diode. The laser had a measured power of 23 mW at $\lambda=658$ nm.[14] Higher-power versions of the module exist in the infrared. These would be more suitable for a research instrument in the lab, particularly if one had biological applications in mind. For an undergraduate lab, it is safer and more practical to use a visible laser source.[15]

B. Microscope

Previous designs have used commercial upright or inverted microscopes or, occasionally, home built inverted microcopes. In our design, we follow the latter course in eliminating the microscope. Not only are good microscopes expensive, but they always introduce the possibility of serious injury to students' eyes if they look through the eyepiece with the trap on. (In normal operation, the beam goes down through the trap and back reflections can readily be removed

by filters. But we need to remember the old adage that anything that can possibly go wrong eventually will.) By eliminating the eyepiece, we eliminate a whole series of unfortunate scenarios. Second, cheap microscopes are often unacceptably floppy when used with the 100X, oil-immersion objectives that produce the best results for trapping. Finally, they are often inflexible when we want to add nonstandard elements to the beam path.

For all of these reasons, we developed an ''open microscope'' based on commercially available optics and mounts, all placed on a standard optical breadboard.[16] Previous designs using such optics have all been ''inverted microscopes,'' with the beam coming up through an objective and onto a horizontal sample stage. In our design, we opted for a *sideways* microscope where the beam path stays parallel to the optical table. This sideways configuration has several advantages:

Keeping the entire beam (laser and microscope) in one plane simplifies greatly the alignment and setup. Once a standard height is chosen (about 10 cm in our setup), one can mark an index card at the proper height and quickly line up all elements approximately to the reference height. Having the microscope beam path at 90° vertical to the laser path is much more difficult to align correctly.

Having a low beam in one plane is safer. Students would have to stoop to put their eyes at the same level as the beam. In the traditional configuration, the beam will almost certainly pass eye level somewhere.

Our microscope design is as follows: The light source is a modified halogen desklamp, whose 20 W bulb puts out ample light.[17] We found that using two plano-convex lenses produced an acceptable condenser. The sample was held on an XYZ translation stage that served to focus and laterally displace the sample. The stage is the most expensive element of the microscope ($650), and a poor choice—one that lacks rigidity or whose movement is not smooth—will lead to much student frustration. After some trial and error, we settled on a 1/2″ stage recently introduced by Thorlabs.[18] As in Ref. 7, we use a student grade 100X oil-immersion microscope objective.[19] Because the lens of the microscope objective and the sample glass slide are vertical, it is important to buy high-viscosity immersion oil.[20]

Finally, the image from the microscope is directly projected onto a camera sensor. We used both a traditional CCD camera[21] producing analog video output and a USB-based Web camera[22] based on a CMOS sensor and producing digital output. (Firewire cameras have recently become available but remain more expensive.) The video camera was fed into a frame grabber[23] and into a computer. Although expensive, the camera and framegrabber provide a robust solution that is easily implemented. Web cameras are much cheaper but less flexible and less durable. They are made of plastic and tend to break and may be in the long run be more expensive to maintain. So many Web cameras are available that it is difficult to examine them all. The one we selected has features that are useful for the present design.

The lens can be removed (and replaced), allowing us to project an image directly onto the CMOS sensor.

The legs detach, allowing us to fasten the camera easily to a standard 1/2″ mounting post.

Other small improvements in our design include the following.

Because the beam is all in one plane, the laser beam encounters only one total-reflecting (''normal'') mirror and one dichroic mirror. (The normal mirror is added only because we need two mirrors to independently fix the position and orientation of the laser beam with respect to the microscope's optical axis.)

Previous designs used two lenses for a beam expander (to make the beam size equal to the back aperture of the microscope objective) and then a third lens to form an intermediate image at the standard 160 mm behind the objective. Here, both functions are accomplished by a single lens. (At the level of paraxial, Gaussian optics, a system of three lenses can always be reduced to a single-lens equivalent.) It is a nice exercise to ask the students to calculate the required focal length of this lens, given the approximate beam diameter from the laser module, the size of the back aperture of the objective, and the standard tube length (160 mm). We find that we should use a lens of focal length $f = 160(D_1/D_2)$ mm, where D_1 is the diameter of the collimated laser beam and D_2 is the diameter of the back aperture of the microscope objective. As Svoboda and Block have noted,[10] it is important to err by overfilling the back aperture, as underfilling will lead to a rapid decrease in effective NA and loss of trapping efficiency.

C. Aligning and operating the trap

Once students have set out all the pieces on the optical breadboard, they are faced with the sometimes frustrating task of aligning the elements to obtain trapping. One basic strategy is to separate the task of building the microscope from that of building the trap. The first step, then, is to align the microscope. This is not too difficult, but we need to make sure that we can make reasonably sharp, isotropic images of spheres in solution. One-micron polystyrene spheres are a good test of the performance of the microscope, and they make good objects to trap, as well.[24] Because their density is close to that of water, spheres less than about 3 μm will settle slowly. To trap larger spheres, we can density match the surrounding fluid by using a water–glycerol mixture. With the smaller spheres, we did not use this technique.

To align the microscope, one trick is to start by identifying the various surfaces (immersion oil–glass, then glass–fluid, then, maybe fluid–glass). Small dust particles in the oil will swirl in a way that differs from the Brownian motion of beads in the fluid. (In particular, the immersion oil flows in direct response to changes in focus, while the fluid inside the sample cell is shielded.)

After the microscope has been aligned, we can introduce the trap via the dichroic mirror. In working on a breadboard with pre-drilled, aligned holes, it is useful to begin by roughly aligning the beam path along the holes. It is also useful to leave out the intermediate lens until the basic alignment has been achieved. Then we can insert the intermediate lens and adjust its position so that the laser beam fills the back aperture.

At this point, we can attempt to trap particles. The basic requirement is that the beam be centered on the optical axis and aligned along it. There are thus four parameters to fix, and four screws on the kinematic mirror mounts. Because the number of ''knobs'' equals the number of variables to adjust, there is a solution. One trick is to note that the horizontal and vertical adjustments are decoupled. Thus, we can simultaneously adjust the horizontal screws of the two mirrors to align the horizontal axis and orientation, before repeating the procedure for the vertical axis. The last adjustment is to

move the intermediate lens along the optical axis in order to make the focus of the trap coincide with the focus of the microscope. Usually, we first reach a situation where the trap is located somewhere inside the glass of the coverslip, so that particles are trapped, in the radial direction by the optical forces and then pinned against the coverslip by the submerged trap. Once trapped in this way, the particles will usually be stuck permanently to the glass. After achieving this situation, we merely have to advance the intermediate lens, so that the trap is pushed up into the fluid.

IV. APPLICATIONS

Although most of the effort in the optical tweezer lab is directed towards setting up and achieving trapping, it is good to have an application as an ultimate goal. Smith *et al.*[7] suggest several possibilities, including the calibration of trap strength by measuring the escape velocity of a trapped particle subjected to a hydrodynamical flow. Moothoo *et al.*[8] discuss the transfer of angular momentum from a circularly polarized beam to an anisotropic particle. In our lab, we ask the students to explore the strength and shape of the trap by looking at the stochastic motion of trapped particles. As discussed below, by making a movie of particle motion, we can deduce the trap strength and even the potential shape. Not only does this exercise give the students some feel for trap properties, it can be an instructive introduction to stochastic phenomena.

Depending on the level and sophistication of students (in particular, whether they have had a course in statistical mechanics), one may explore these issues in different depth. We will discuss first a simple version that is suitable for third-year students who have not had any statistical mechanics and then a more complete version that raises subtle issues.

A. Simple analysis of trapped-particle statistics

The basic measurement is to take a movie of the bead caught in the trap and to use the equipartition theorem to deduce the trap strength. In doing so, we are approximating the shape of the trap potential by a parabola, as illustrated schematically in Fig. 2(a). We use standard software packages to record a movie of at least 100 images of a trapped bead, storing it to a hard disk. If the software permits, one should record a cropped image that just encloses the bead (50 by 50 pixels often suffices); otherwise, one may crop the movie afterwards to reduce file size and to aid in the image processing.

We have written routines in NIH/Scion Image to extract the bead position from a movie that is cropped to include the image of the fluctuating bead and nothing else.[25] Once we have a list of x and y positions for the bead, we can use the equipartition theorem,

$$\tfrac{1}{2}k_x\langle x^2\rangle = \tfrac{1}{2}k_BT, \tag{8}$$

where k_x is the trap spring constant for displacements along the x axis, x is the *deviation* of the particle from its mean position x_0, $\langle\cdots\rangle$ denotes averages over the N measurements in the movie, k_B is Boltzmann's constant, and T is the absolute temperature. Equation (8) holds only to the extent that part of the potential that the bead explores can be approximated as parabolic. Making such an approximation allows us to simply use the variance of the measured positions to obtain the trap spring constant. We can then repeat the measurements for the y axis and for different laser powers.[26] (Because the laser output is polarized, the power may be conveniently reduced using an analyzer set at a variable angle.) From Eq. (8), we expect that the graph of variance versus $1/P$ should be linear, where P is the laser power. (The linearity of Maxwell's equations and the constitutive equations implies that $k_x \propto P$.) Typical data are shown in Fig. 3(a). Note that the infinite-power limit does not extrapolate to zero variance. The extra fluctuations can be traced to the effect of shot noise in the images, which produces apparent positional fluctuations. They are minimized by selecting as many pixels as possible in the threshold algorithm.[25] Because this noise is independent of the bead's random movements, we can simply subtract its variance to estimate the spring constant versus power (again assuming a linear restoring force on the bead) [see Fig. 3(b)].

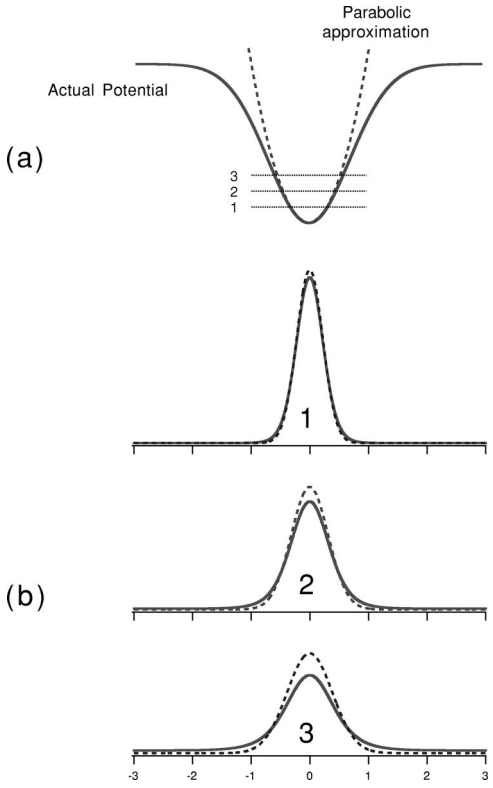

Fig. 2. (a) Schematic of potential well seen by trapped particle. Solid line is the actual potential; dashed line is parabolic approximation. (b) Position distributions for three different temperatures (1, 2, and 3), as shown by horizontal lines in (a). Note how the distributions broaden as the temperature increases from 1 to 3. Note, too, the increasing difference between the parabolic approximation, which leads to a Gaussian, and the actual distribution.

B. More complete analysis of trapped-particle statistics

If the level of the students and the time available permit, there are many issues ignored in the simple analysis presented above that can be explored.

The trap potential was assumed to be parabolic, whereas in fact it should flatten out far away from the beam focus [Fig. 2(a)]. We can in principle detect deviations from the parabolic shape by computing the Boltzmann distribution,

$$\rho(x) = \frac{1}{Z}e^{-U(x)/k_BT}, \tag{9}$$

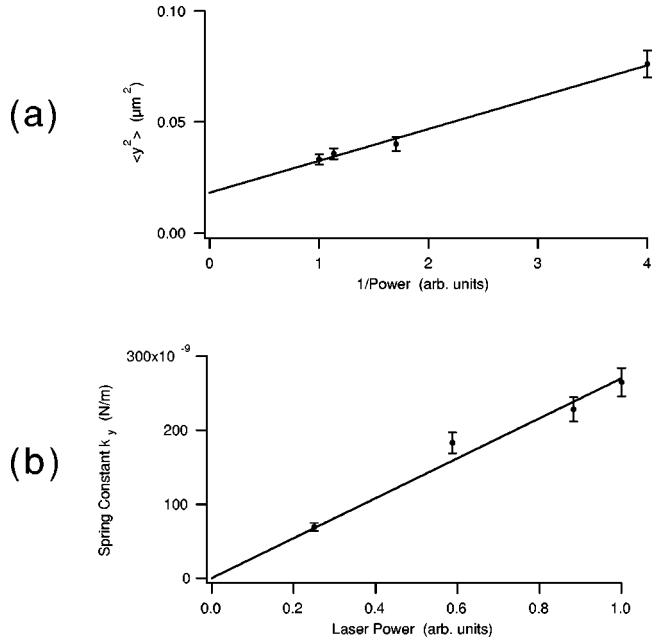

Fig. 3. (a) Position variance versus $1/P$. (b) Spring constant versus P. Error bars in (a) were obtained from a Monte Carlo simulation of the data sets. Fit in (b) was forced through 0.

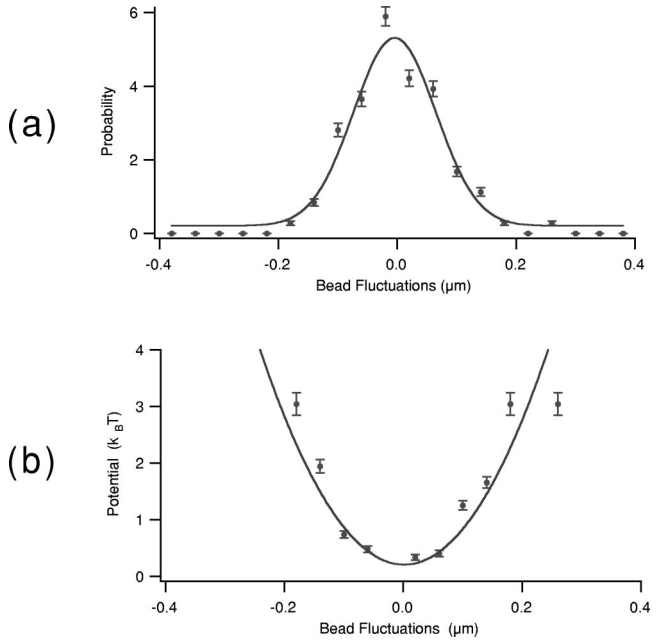

Fig. 4. (a) Observed distribution of particle positions for one-dimensional displacements in the trap. The distance scale was calibrated by using the micrometers on the XY part of the translation stage to make known displacements of particles stuck to the glass plates. The observed distribution is roughly Gaussian. As explained in the text, the observed distributions are convoluted with a Gaussian distribution of measurement errors. The true distributions would be narrower. (b) Potential inferred from (a) using the Boltzmann distribution.

where the partition function Z is defined so that $\int_{-\infty}^{\infty}\rho(x)dx=1$. For a parabolic potential, the expected distribution is Gaussian, and the equipartition theorem holds. The expected potential shape will have broader wings, because the particle will spend more time in the wings of the potential. This evolution of particle-position distribution with temperature is illustrated in Fig. 2(b), for three different temperatures, showing the increasing deviations as the trap becomes weaker (1 to 3). (The normalization of a potential that is finite for large deviations raises some even more subtle points.[27]) A typical measured distribution is shown in Fig. 4(a). To date, we have not been able to detect convincing deviations from a Gaussian [cf. Fig. 4(b)], but with enough images, the detection of such deviations should be possible. (As computers and cameras improve, the 100 or so images that we have recommended that students take can be increased.)

The observations have been heretofore been assumed to be independent. A more careful statement is that particle positions are correlated over a time scale τ_0 that has been assumed to be shorter than the time interval between movie frames. In order for the simple analysis described above to make sense, each individual snapshot should have an exposure time $\ll\tau_0$ while the interval between snapshots should be $\gg\tau_0$. The former condition is easy to satisfy in cameras with electronic shutters, which often can be as fast as 10^{-4} s. The latter condition is usually satisfied for a strong trap. In the Appendix, we show that the autocorrelation function for positional fluctuations is given by

$$\langle x(t)x(t+\tau)\rangle=\frac{k_BT}{k}e^{-|\tau|/\tau_0}, \tag{10}$$

with the correlation time $\tau_0=\gamma/k$, where γ is the fluid damping and k the spring constant. Thus, as the laser power (and hence spring constant) tends to zero, τ_0 becomes large, and the standard video capture rates may lead to correlated measurements.

How can we deal with correlated measurements? The easiest way is to retake the time series, taking care to lengthen the time interval between frames sufficiently beyond the correlation time. We return then to the simple situation mentioned above. If we cannot change the capture rate, we can simply select images at long-enough intervals, throwing out the rest of the data. Doing anything more sophisticated is probably not worth the effort. Ambitious students can measure τ_0 and deduce the spring constant that way. They should compare their result to that obtained from the equipartition theorem.

As discussed already in the simple version of the analysis, shot noise in the image produces readily measurable fluctuation noise in the measurement position. If the trapping potential is Gaussian, we can treat this complication in the simple way described above. Because the shot-noise-induced fluctuations are independent of the fluctuations in the bead's movement, we can simply subtract the variance of the shot-noise fluctuations from the total variance to recover the true variance that is needed in Eq. (8), thereby justifying the construction used in Fig. 3(b).

If the trap potential is not Gaussian, then the observed positional histogram $\rho_{\rm obs}(x)$ will be the convolution of the desired particle $\rho_{\rm true}(x)$ with distribution $\rho_{\rm shot}(x)$ that describes the effect of shot-noise fluctuations on the inferred position of the particle:

$$\rho_{\rm obs}(x)=\int_{-\infty}^{\infty}dx'\,\rho_{\rm true}(x')\rho_{\rm shot}(x-x'). \tag{11}$$

It is safe to assume (and we can verify by looking at positional fluctuations in the high-power limit) that $\rho_{\text{shot}}(x)$ is Gaussian. The measurement variance is given by the intercept in Fig. 3(a). We are thus faced with a classic inversion problem: Given ρ_{obs} and ρ_{shot}, find ρ_{true}. There are many techniques for solving such a problem.[28] The naive way is to write down a finite representation and invert the response matrix. Because of noise, inversion is usually a poor algorithm, which leads to unacceptably large fluctuations in the estimate for ρ_{true}. The other ways to proceed all involve imposing *a priori* knowledge of the smoothness of the distribution ρ_{true} to constrain the space of possible solutions. Cowan,[28] for example, discusses Tikhonov and maximum-entropy regularization, which take into account prior information in different ways. The methods are probably too complicated for a lab course—unless one has access to canned routines. In any case, it is important to recognize the distinction between the fatter, more Gaussian-looking ρ_{obs} and the actual distribution ρ_{true}.

V. CONCLUSIONS

We have introduced a design for optical tweezers that is suitable for a third- or fourth-year undergraduate physics laboratory. In particular, it is faster to set up, cheaper, and, we believe, safer than previous designs. Students in our course take three 4-hour sessions to complete the laboratory. The stochastic analysis of the motion of the trapped particle is attractive because it is one of the few places in the undergraduate curriculum where a student can experiment with stochastic phenomena, at readily accessible space and time scales. Moreover, the analysis can be done with varying degrees of sophistication, as appropriate to the level of the students and the amount of time that they have.

ACKNOWLEDGMENTS

We thank Laura Schmidt, Jeff Rudd, and Mehrdad Rastan for all the help they gave us in overcoming various technical problems. We thank the students in Physics 332 for their enthusiasm (and, occasionally, patience) in helping to debug a new and sometimes tricky experiment. J.B. thanks the Charpak–Vered Foundation and NSERC for support during a sabbatical leave which gave the chance to learn about optical tweezers and some of the wonderful things that they can do. J.B. also thanks Joel Stavans, Dept. of Complex Systems, Weizmann Inst. (Israel) for welcoming me into his laboratory and giving the chance to build a first setup. The present setup was built with teaching funds from Simon Fraser University.

APPENDIX

As mentioned above, there is a characteristic time scale, τ_0, for thermal fluctuations of a particle trapped in a potential. If observations are made on scales much longer than τ_0, they may be treated as independent measurements of the position. If not, one must worry about correlations. Here, we give some details about this problem, following methods originally due to Langevin. The general issues are described in the commonly used statistical physics textbook by Reif.[29]

Consider a particle immersed in a fluid and trapped in a harmonic potential. The particle is small enough that thermal fluctuations are visible but much larger than the fluid molecules. Its equation of motion is

$$m\ddot{x}+\gamma\dot{x}+kx=\xi(t), \tag{A1}$$

where m is the particle mass, x the deviation from equilibrium, γ the friction coefficient, k the trap spring constant, and $\xi(t)$ the fluctuating force due to random kicks by the many neighboring fluid molecules. We will discuss the properties of ξ below. If the particle is a sphere of radius R immersed in a fluid of viscosity η and far from any boundaries, then standard hydrodynamic arguments lead to $\gamma=6\pi R\eta$.

One simplification is that in all cases we are interested in, the motion is so overdamped that one may neglect completely the inertial term in Eq. (A1), giving

$$\dot{x}+\frac{1}{\tau_0}x=\frac{1}{\gamma}\xi(t), \tag{A2}$$

where $\tau_0=\gamma/k$ is the relaxation time. We can treat $\xi(t)$ as an arbitrary driving function and solve Eq. (A2), finding

$$x(\tau)=e^{-\tau/\tau_0}\int_{-\infty}^{t}\frac{1}{\gamma}\xi(\tau')e^{\tau'/\tau_0}\,d\tau'. \tag{A3}$$

In order to construct the correlation function $\langle x(t)x(t+\tau)\rangle$, we write

$$x(0)x(\tau)=\frac{e^{-\tau/\tau_0}}{\gamma^2}\int_{-\infty}^{0}\xi(\tau'')e^{\tau''/\tau_0}\,d\tau''\int_{-\infty}^{\tau}\xi(\tau')e^{\tau'/\tau_0}\,d\tau'. \tag{A4}$$

The autocorrelation function is then obtained by taking an ensemble average, bearing in mind that the only stochastic (random) terms are the ξ's:

$$\langle x(0)x(\tau)\rangle=\frac{e^{-\tau/\tau_0}}{\gamma^2}\int_{-\infty}^{0}d\tau''\int_{-\infty}^{\tau}d\tau'\,\langle\xi(\tau')\xi(\tau'')\rangle e^{(\tau'+\tau'')/\tau_0}. \tag{A5}$$

Next, we assume that

$$\langle\xi(\tau')\xi(\tau'')\rangle=M\delta(\tau'-\tau''), \tag{A6}$$

where δ is a Dirac delta function and M is an amplitude, to be determined below. Physically, the assumption of the delta-function form means that successive random kicks are uncorrelated with each other, or, more precisely, that any correlations take place on time scales $\tau\ll\tau_0$. (This time scale would typically be a phonon frequency, about 10^{-13} s, quite a short time indeed.)

Continuing the derivation, we have

$$\langle x(0)x(\tau)\rangle=\frac{M}{\gamma^2}e^{-\tau/\tau_0}\int_{-\infty}^{0}d\tau''\int_{-\infty}^{\tau}d\tau'\times\delta(\tau'-\tau'')e^{(\tau'+\tau'')/\tau_0} \tag{A7}$$

$$=\frac{M}{\gamma^2}e^{-\tau/\tau_0}\int_{-\infty}^{0}d\tau''\,e^{(2\tau'')/\tau_0} \tag{A8}$$

$$=\frac{M}{\gamma^2}\frac{\tau_0}{2}e^{-\tau/\tau_0}=\frac{M}{\gamma^2}\frac{\gamma}{2k}e^{-\tau/\tau_0}=\frac{M}{2\gamma k}e^{-\tau/\tau_0}. \tag{A9}$$

Now, the equipartition theorem states that $\langle x^2\rangle=k_BT/k$, and thus

$$M = 2k_B T\gamma. \tag{A10}$$

The final form of the autocorrelation function is then

$$\langle x(t)x(t+\tau)\rangle = \frac{k_B T}{k} e^{-|\tau|/\tau_0}, \tag{A11}$$

where the absolute value can be established either by considering the explicit case $\tau<0$, or more generally, by noting that the autocorrelation function of a real function is always even. Note that we have replaced 0 by t, which is allowed because we are assuming that $x(t)$ is a stationary stochastic process, so that ensemble averages are independent of the time at which they are carried out.

Thus, as claimed, correlations last a time $\tau_0 = \gamma/k$. When the laser power (and thus, trap strength k) is low, the correlation times can be long and must be taken into account. The finite correlation time can also be interpreted as a kind of low-pass filtering by the particle of the original white noise and, indeed, Fourier methods are often preferred for discussing these types of stochastic problems. Using the Wiener–Khintchine theorem, one can calculate the power spectrum of the particle by taking the Fourier transform of Eq. (A11). One finds

$$x^2(\omega) = \frac{2k_B T\gamma}{k^2(1+\omega^2\tau_0^2)}, \tag{A12}$$

which gives the characteristic frequency response of the particle to the thermal driving force, normalized so that $\int_0^\infty x^2(\omega)d\omega = k_B T/k = \langle x^2\rangle$. In addition, we have established the strength M of the thermal noise in Eq. (A10). The result is at first surprising, because in addition to $k_B T$, there is a factor of γ, the dissipation. This relation is a simple example of the fluctuation-dissipation theorem, described also in Reif.[29]

Finally, it is interesting to estimate some numbers. For a 1 μm diameter particle in water ($\eta \approx 10^{-3}$ kg/m s), $\gamma \approx 10^{-8}$ (MKS). A typical trapping force is of order Pn/c,[7] with laser power $P \approx 10$ mW for a strong trap, medium index $n = 1.33$, and c the velocity of light. This gives a trap strength ≈ 10 pN and a typical spring constant ≈ 10 pN/1 μm $= 10$ μN/m, implying a relaxation time $\tau_0 \approx 1$ ms. Weaker traps will have slower time scales, and one needs to wait 2–3 τ_0 to be able to neglect correlations completely. If one acquires data at video rates and the trap is weak, one can see correlations easily.

[a]Author to whom correspondence should be addressed. Electronic mail: johnb@sfu.ca

[1]A. Ashkin, J. M. Dziedzic, J. E. Bjorkholm, and Steven Chu, "Observation of a single-beam gradient force optical trap for dielectric particles," Opt. Lett. **11**, 288–291 (1986).

[2]S. B. Smith, Y. Cui, and C. Bustamante, "Overstretching B-DNA: The elastic response of individual double-stranded and single-stranded DNA molecules," Science **271**, 795–799 (1996).

[3]K. Svoboda, C. F. Schmidt, B. J. Schnapp, and S. M. Block, "Direct observation of kinesin stepping by optical trapping interferometry," Nature (London) **365**, 721–727 (1993).

[4]M. Rief, R. S. Rock, A. D. Mehta, M. S. Mooseker, R. E. Cheney, and J. A. Spudich, "Myosin-V stepping kinetics: A molecular model for processivity," Proc. Natl. Acad. Sci. U.S.A. **97**, 9482–9486 (2000).

[5]R. Bar-Ziv, E. Moses, and P. Nelson, "Dynamic excitations in membranes induced by optical tweezers," Biophys. J. **75**, 294–320 (1998).

[6]Sylvie Hénon, Guillaume Lenormand, Alain Richert, and François Gallet, "A new determination of the shear modulus of the human erythrocyte membrane using optical tweezers," Biophys. J. **76**, 1145–1151 (1999).

[7]Stephen P. Smith, Sameer R. Bhalotra, Anne L. Brody, Benjamin L. Brown, Edward K. Boyda, and Mara Prentiss, "Inexpensive optical tweezers for undergraduate laboratories," Am. J. Phys. **67**, 26–35 (1999).

[8]D. N. Moothoo, J. Arlt, R. S. Conroy, F. Akerboom, A. Voit, and K. Dholakia, "Beth's experiment using optical tweezers," Am. J. Phys. **69**, 271–276 (2001).

[9]R. Pastel, A. Struthers, R. Ringle, J. Rogers, C. Rohde, and P. Geiser, "Laser trapping of microscopic particles for undergraduate experiments," Am. J. Phys. **68**, 993–1001 (2000).

[10]K. Svoboda and S. M. Block, "Biological applications of optical forces," Annu. Rev. Biophys. Biomol. Struct. **23**, 247–285 (1994).

[11]A. Ashkin, "Forces of a single-beam gradient laser trap on a dielectric sphere in the ray optics regime," Biophys. J. **61**, 569–582 (1992).

[12]T. Tlusty, A. Meller, and R. Bar-Ziv, "Optical gradient forces of strongly localized fields," Phys. Rev. Lett. **81**, 1738–1741 (1998). Note that the Gaussian form for the beam shape [Eq. (4)] is inaccurate in that it assumes a Gaussian fall-off along the beam axis, whereas the actual intensity decreases asymptotically as z^{-2}. But both the true form and the assumed form vary quadratically about the focus, and the behavior there dominates in the calculation of trapping forces.

[13]Because of typographical errors in their version of our Eqs. (6) and (7), the formulas for trapping constants given in Ref. 12 were incorrect. The correct formulas, however, were used in calculating the results given in Ref. 12. [A. Meller and T. Tlusty (private communication).]

[14]Power Technology, PMP (LD1240) laser diode module, LDCU5 power supply, and PM–ACS–HS heat sink ($500). The setup is based on a Blue Sky Research circu-laser module. Note that although the laser itself is advertized as producing 35 mW, the feedback loop used to stabilize the optical power reduces this somewhat. We measured 23 mW for our module.

[15]The design of Moothoo *et al.* (Ref. 8) uses the infrared Blue-Sky laser.

[16]The breadboard and kinematic lens and mirror mounts are standard grade parts from Thorlabs, Inc. We used a 24-by-36 inch breadboard, which is larger than needed for this experiment. One could use an 18-by-24 inch board, but the extra space makes the layout easier and makes the board more useful for other experiments. The breadboard and kinematic mounts are available from a wide range of suppliers, almost all of which will be suitable.

[17]Ikea Expressivo lamp ($8). We modified the commercial lamp by replacing the two metal rods that connect base to lamp head with a two-wire cable. The head was attached to a standard post for mounting to the table and extra slots were cut to ensure cooling. We also added a light shield to block stray light.

[18]Thorlabs, Model MT3. Note that their 1 in. stage (Model PT3) was much less rigid and had a movement that was much more prone to stick-slip motion.

[19]Edmund Scientific, 100X Achromat, K43-905 ($95).

[20]Edmund Scientific, high-viscosity immersion oil, CR38-503 ($9).

[21]Pulnix, model TM-7CN ($550).

[22]Irez Corp., Kritter USB ($100). A Firewire version costs $200.

[23]Scion Corp., LG-3 ($900). The Macintosh PCI-bus version can digitize up to 30 frames (60 fields) per second directly into memory.

[24]Interfacial Dynamics Corp, `http://www.idclatex.com`, NIST-size-standard spheres. Adding a small amount of surfactant (for example, 1% TWEEN) can help prevent spheres from sticking to each other. A similar amount of sodium azide will prevent bacterial growth if samples are going to be used over long periods of time (months). Note that microspheres available from other suppliers (Duke, Bangs, etc.) will be equally satisfactory.

[25]NIH Image is a freely available image-processing software package for Macintosh computers. (`http://rsb.info.nih.gov/nih-image/index.html`) A Windows version, Scion Image, is also freely available (`http://www.scioncorp.com/`). The macro routines we use in processing the images are also available in EPAPAS Document No. EPAPS-AJPIAS-70-009203. This document may be retrieved via the EPAPS homepage (http://www.aip.org/pubservs/epaps.html) or from ftp.aip.org in the directory /epaps/. See the EPAPS homepage for more information. The basic strategy we use is to threshold the image so that the selected pixels lie entirely in the bead image and move along with it. The position is extracted by computing the x and y centers of mass of the pixels. A weakness of this method is that variations in the background intensity can produce spurious position shifts. We thus include a routine that normalizes each image by the average intensity of all pixels. A rule of thumb is that the better the original image, the better these routines work.

Also, as shown in Fig. 3(a), there are residual fluctuations observed even for stationary objects. These are due to shot-noise fluctuations, which produce apparent positional fluctuations.

[26]Note that although it is easy to get relative power measurements, it is quite difficult to measure accurately the power actually delivered to the trap. The beam spreads out extremely rapidly from the trap, so much so that another objective would be required to collimate the beam. However, there are significant losses from each objective and the first objective may block an unknown fraction of the beam. The power measured at the output of the second objective is thus not a reliable measurement of the power at the trap. Another approach is to measure the portion of the power that falls on the light-meter detector as a function of the distance of the active surface from the objective and to extrapolate back to zero distance. However, this method is sensitive to misalignments of the detector's center from the optical axis and, in practice, is difficult to do well. In our lab, we have merely asked students to try to place upper and lower bounds on estimates for the actual power delivered to the trap.

[27]The normalization of a finite-depth potential is tricky. The naive thing to do is to calculate the partition function Z as $\lim_{X\to\infty}\int_{-X}^{X} d(\delta x)\,\rho(\delta x)$, but taking this limit just gives a uniform distribution, with the particle equally likely to be in any particular range of δx. (The ''bump'' of extra probability at the center disappears as the limit is taken.) The problem is that in equilibrium, essentially all particles will have escaped the potential and will wander over the real axis. What one wants is the probability distribution of a particle that stays trapped in the potential and does not escape. In other words, we suppose a separation of time scales, so that the time to thermalize within the potential trap is much shorter than the observation time and also than the time to escape. For traps deeper than a few k_BT, this condition will hold.

[28]G. Cowan, *Statistical Data Analysis* (Oxford University Press, New York, 1998), Chap. 11.

[29]F. Reif, *Statistical and Thermal Physics* (McGraw-Hill, New York, 1965), Chap. 15, especially Secs. 6 and 10.